A R C H I V E S O F M E T A L L U R G Y A N D M A T E R I A L S
Volume 54 2009 Issue 3

T. GORYCZKA*

EFFECT OF WHEEL VELOCITY ON TEXTURE FORMATION AND SHAPE MEMORY IN Cu-Al-Ni BASED MELT-SPUN RIBBONS

WPŁYW SZYBKOŚCI OBROTOWEJ BĘBNA CHŁODZĄCEGO NA FORMOWANIE SIĘ TEKSTURY W STOPACH NA BAZIE CU-AL-NI WYKAZUJĄCYCH EFEKT PAMIĘCI KSZTAŁTU WYTWARZANYCH METODĄ MELT-SPINNING

The Cu-Al-Ni-Mn and Cu-Al-Ni-Ti shape memory alloys were melt-spun from 1250°C applying different combination of the wheel velocity (from 12 m/s up to 26 m/s). The texture consists mainly of the <100> fibre component and two sheet components orientation: {100}<001> or/and {100}<011> in the Cu-Al-Ni-Mn ribbons. In a case of the Cu-Al-Ni-Ti ribbons spun with 12m/s or 19m/s only <100> fibre component and sheet texture {100}<011> were observed. However, increase of the wheel velocity up to 26m/s causes formation of the <111> and {111}<112> textural components. The grains orientation significantly influenced the shape recovery measured as a change of elongation under constant load during thermal cycling. The maximum of recoverable strain under constant tensile load was 5,8% and 6,2% for Cu-Al-Ni-Mn and Cu-Al-Ni-Ti alloy, respectively.

Keywords: texture, shape memory effect, shape recovery, Cu-based shape memory alloys, martensitic transformation

Stopy Cu-Al-Ni-Mn oraz Cu-Al-Ni-Ti wykazujące efekt pamięci kształtu wytworzono metodą szybkiego schładzania z fazy ciekłej w układzie pojedynczego bębna chłodzącego. Odlano serię taśm z temperatury 1250°C stosując różne szybkości obrotowe bębna od 12m/s do 26m/s. Tekstura w taśmach stopu Cu-Al-Ni-Mn składała się ze składowej osiowej < 100 > oraz dwóch składników tekstury pełnej: {100}<001> i {100}<011>. W przypadku taśm stopu Cu-Al-Ni-Ti odlewanych stosując obroty bębna 12m/s i 19m/s stwierdzono obecność tylko dwóch składowych tekstury <100> oraz {100}<011>. Jednakże zwiększenie obrotów bębna do 26m/s spowodowało uformowanie składowych <111> oraz {111}<112>. Orientacja ziaren znacząco wpłynęła na odzysk kształtu zmierzony jako wydłużenie w trakcie zmian temperatury przy stałym obciążeniu rozciągającym. Najwyższą wartość wydłużenia, jaką uzyskano w taśmach stopu Cu-Al-Ni-Mn to 5,8% natomiast 6,2% w taśmach Cu-Al-Ni-Ti.

1. Introduction

Ternary Cu-Al-Ni shape memory alloys are known from their good thermal and electrical conductivity, high transformation temperatures, good thermal stability of the martensitic transformation as well as large recoverable strain [1-3]. Taking into account their practical application the last property is especially important. Bhattacharya et. al. [4], basing on theoretical crystallographic approach of structure transformation from the parent phase to martensite, shown that the maximum of recoverable strain can reach 10,1%. In practice, this value can reach 9% dependently on the orientation of a single crystal, whereas in case of textured polycrystals – 6,5% [5]. However, polycrystals are brittle and reveal tendency to intergranular fractures [6]. In order to overcome such inconvenience various technologies of shape memory alloys (SMA) manufacturing, leading to grain refinement as well as texture formation, were applied. One of them is melt-spinning (MS). It appeared to be a useful technique for production of ribbons, which reveal shape memory effect [5, 7-9]. However, physical properties of the melt-spun ribbons as well as behavior of the martensitic transformation depend on several processing parameters: wheel velocity, melt temperature, ejection pressure, diameter of a wheel, diameter of a nozzle, distance between nozzle and wheel, ect.

The transformation behavior and consequently shape memory effect can also be modified by change of the chemical composition. It was reported that addition of the forth or fifth alloying element, as a substitution in the Cu-Al-Ni alloy significantly influenced the martensitic transformation. General behavior and stabilization of the martensitic transformation in quaternary melt-spun ribbons: Cu-Al-Ni-Mn and Cu-Al-Ni-Ti as well as quinary Cu-Al-Ni-Ti-B alloys were reported

* INSTITUTE OF MATERIALS SCIENCE, UNIVERSITY OF SILESIA, 40-007 KATOWICE, 12 BANKOWA STR., POLAND

in [7-12]. Goryczka et. al. [10] showed that annealing of Cu-Al-Ni-Ti-B ribbons can increase maximum recoverable strain up to 4.5% measured at constant tensile stress of 30MPa. Malarria et. al. [13] compared properties of the melt-spun ribbon and twin rolls cast strips for Cu-Al-Ni-Ti alloy. After thermal treatment the maximum elongation was 1,8% applying external tensile stress of 90MPa. However, for the practical application, full characterization of the shape recovery up to stress, which causes plastic deformation, is required.

The aim of presented work was to study influence of the texture on the shape recovery in quaternary Cu-Al-Ni-Mn and Cu-Al-Ni-Ti melt-spun ribbons. Different texture components were obtained by applying different wheel velocity during the ribbon solidification. Also, dependence of the martensitic transformation on solidification rate was characterized. In order to show influence of additional alloying elements: Mn and Ti on course of the martensitic transformation bulk alloy of ternary Cu – 13wg%Al – 4wg%Ni composition was used. Characterization of the Cu-Al-Ni melt spun ribbons can be found at [11].

2. Experimental procedure

The ribbons of quaternary Cu-Al-Ni-Mn and Cu-Al-Ni-Ti shape memory alloys were produced by melt-spinning technique. The bulk alloys, with nominal chemical composition given in Table 1, were induction melted under helium gas atmosphere and then the ribbons were cast in a vertical caster. For studies, the bulk alloys were homogenized at 900°C for 1h and quenched to the water. The ribbons were cast from the melt temperature of 1250°C applying the wheel velocity of 12 m/s, 19 m/s or 26 m/s. Dependently on casting parameters, average thickness of the ribbons varied from 30 up to 60μm and width from 6 to 10mm.

Temperatures of the martensitic transformation were determined from measurement carried out using Perkin Elmer differential scanning calorimeter (DSC). In order to receive sample weight of 50 mg, several discs, 4 mm in diameter, were cut from the ribbons and encapsulated in aluminium pans.

TABLE 1
Nominal chemical composition of the bulk alloys

Symbol	Cu [wg%]	Al [wg%]	Ni [wg%]	Mn [wg%]	Ti [*wg*%]
53	81,2	11,8	4,0	3,0	–
55	82,3	13,5	3,2	–	1

Microstructure of the bulk alloys as well as the ribbons was observed using transmission electron microscope the JEM 3010 as well as scanning electron microscope the JEOL 6480.

The pole figures were recorded applying Philips PW1130 diffractometer with texture goniometer by reflection mode to the maximum tilting angle 80°. The ribbons were fixed in a sample holder along their length in such manner, that RD direction was always parallel to length of the ribbon. Three pole figures were measured {111}, {110} and {100}. The indexes are given in the DO_3 structure description. From measured pole figures the orientation distribution function (ODF) was calculated. Identification of the texture components and quantification of the volume fractions were done using LaboTex computer program [14].

Shape memory effect was studied by means of shape recovery measured as an elongation versus temperature change under constant tensile stress. Stress was applied along the length of the ribbon. For each loaded sample 4 to 10 thermal cycles were done. After that stress was increased of 10 or 20 MPa for a next cycle. Measurements were repeated till appearance of plastic deformation. As a result of this, the thermal loops are not closed. Shape recovery was calculated as a difference between maximal elongation and permanent elongation. If permanent elongation equals zero, the hysteresis loop is closed, it means that the shape recovery is equal to the maximal elongation.

3. Results and discussion

3.1. Transformation behaviour in as-cast state

The transformation in shape memory alloys occurs from the high temperature parent phase to the martensite. In a case of the Cu-based alloys, structure of the β_1 parent phase can be ordered with superlattice of B2 or DO_3 type. Independently on the crystal structure of the parent phase, it transforms to the 18R and/or 2H martensite. Transformation temperatures of the bulk alloys and the ribbons were determined from DSC cooling/heating curves. The temperatures were denoted as follow: M_s – start of the forward martensitic transformation, M_f – end of the forward martensitic transformation, A_s – start of the reverse martensitic transformation and A_f – end of the reverse martensitic transformation. Figure 1a shows comparison of the M_s, M_f, A_s, and A_f temperatures calculated for the bulk alloys. The highest values were received for the Cu-Al-Ni alloy. The martensitic transformation occurred in the thermal range between 146°C and 163°C. Lowering Cu content of about 1wg% and simultaneously adding 1%wg of Ti leads to significant decrease of the transformation temperature of 50 degrees. Further lowering of the transformation temperatures was

noticed for the Cu-Al-Ni-Mn alloy, in which the transformation temperatures decreased of 100 degrees in comparison to the Cu-Al-Ni alloy. However, thermal range of the transformation, calculated as a difference between the A_f and M_f temperatures, increased from 17 to 33 degrees. Simultaneously, the transformation enthalpies decreased their values from 7 J/g to 6,1 J/g and 5,3 J/g for Cu-Al-Ni, Cu-Al-Ni-Ti and Cu-Al-Ni-Mn the bulk alloys, respectively (Figure 1b). It can be caused by presence of precipitates observed in the bulk alloys. The precipitates form local stress fields, which act as an obstacle for the formation of the martensitic plates. Moreover, the precipitations process lowers amount of the transformable phase. In consequence, it lowers the transformation enthalpy. In a case of the Cu-Al-Ni-Ti alloy the X-phase precipitates were observed (Figure 2a) whereas in the Cu-Al-Ni-Mn particles of the γ_2-phase were found (Figure 2b).

a)

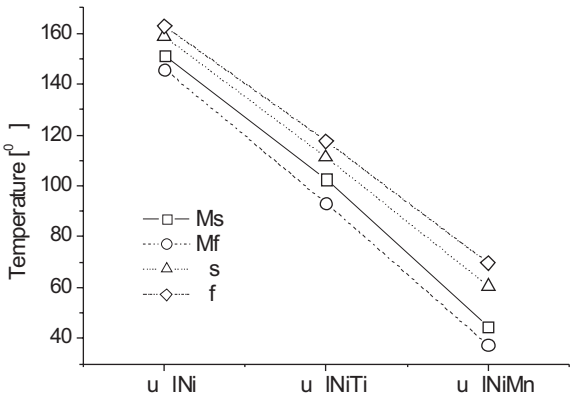

b)

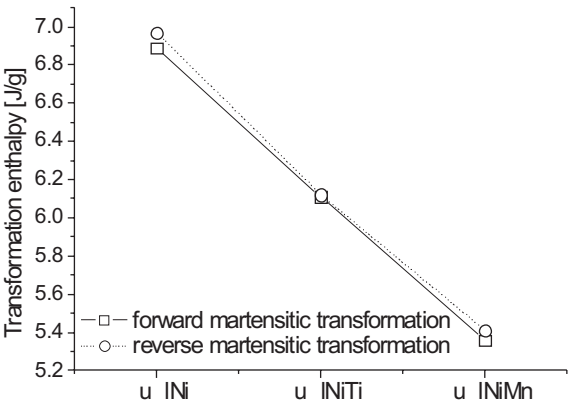

Fig. 1. Transformation temperatures and enthalpy determined for the bulk alloys

Transformation behaviour of the ribbons significantly depends on processing parameters. The most important factor is the wheel velocity. Its influence on the transformation temperatures is shown in Figure 3. It can be clearly seen that in the ribbons spun with speed of 12m/s the transformation temperatures decreased of 70 and 20 degrees for Cu-Al-Ni-Ti and Cu-Al-Ni-Mn, respectively. Further increase of the wheel velocity up to 26 m/s caused decrease of the transformation temperatures of 21 and 32 degrees for the Cu-Al-Ni-Ti and Cu-Al-Ni-Mn ribbons, respectively. Opposite to that, the thermal range of the martensitic transformation increased from 66 to 81 degrees for the Cu-Al-Ni-Ti ribbon and from 41 up to 67 degrees in the Cu-Al-Ni-Mn ribbon. Such behaviour can be explained by additional modification of the microstructure introduced during rapid solidification. Due to the high cooling rate the grains size is reduced. Decrease of the grain size causes decrease of the transformation temperatures. Also, rapid solidification increases density of quenched-in structural defects, such as point defects and/or dislocations, much more than in the bulk alloys. Figure 2c shows relatively high density of dislocations observed the Cu-Al-Ni-Mn ribbon. Presence of the defects requires additional lowering of the M_f temperature to complete the martensitic transformation. Such effect was already reported by Morawiec et al [15]. In highly deformed NiTi alloy, dislocations formed net in the region close to the grains borders. In consequence, the transformation temperatures decreased and the transformation occurred in two stages. Pons et al [7] showed that thermal cycling of a Ni-Ti-Co melt-spun ribbon increased density of dislocation and transformation temperature decreased. Also the precipitates observed in the bulk alloys were appeared in the ribbons.

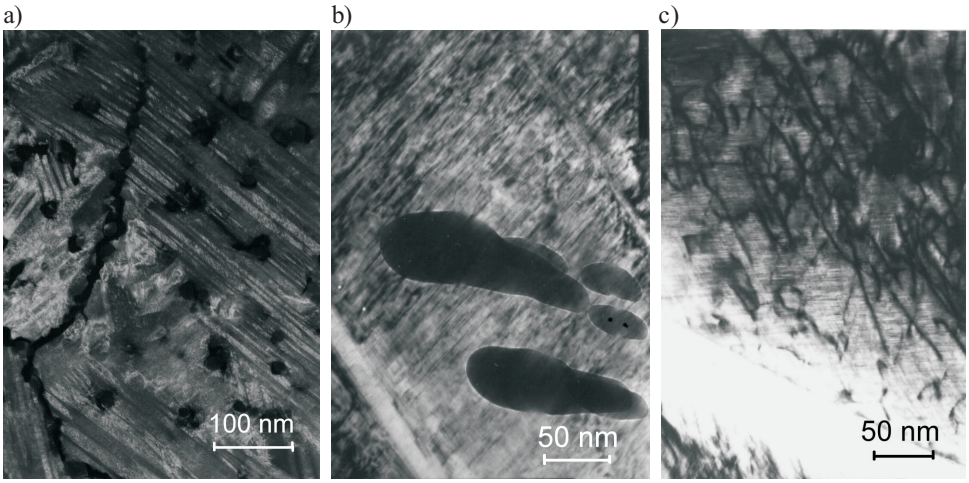

Fig. 2. Precipitates observed in the Cu-Al-Ni-Ti (a) and Cu-Al-Ni-Mn (b) bulk alloys and dislocation in the Cu-Al-Ni-Mn ribbon (c)

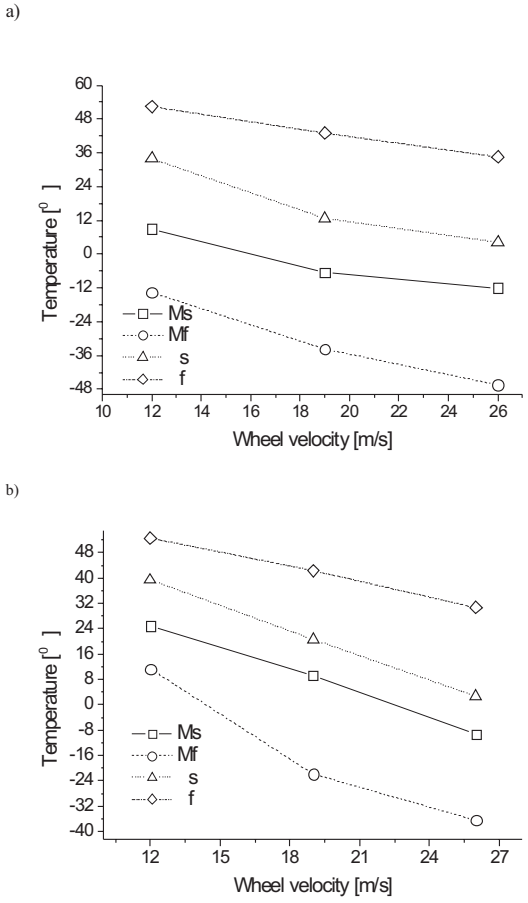

Fig. 3. Transformation temperatures versus wheel velocity for the ribbons: Cu-Al-Ni-Ti (a) and Cu-Al-Ni-Mn (b)

3.2. Texture

During solidification of the ribbon, the crystallization starts from the side, which is in direct contact with rotated wheel. First, a zone, having a contact with rotating wheel, crystallizes and then an outer surface of the ribbon is formed. This zone is about 10 micrometers thick. As an example, fractures perpendicular to the length of the Cu-Al-Ni-Ti ribbons spun using wheel velocity of 12 m/s and 26 m/s are shown in Figure 4. The heat, which flows in opposite direction to the grains growth, forms their columnar shape. In case of the ribbons spun at 26 m/s, columnar grains are tilted not only along the length of the ribbons but also across. High cooling rate close to the rotating wheel caused, that the zone formed at contact side consists of fine grains. Greater part of these grains is randomly oriented. This effect is better distinguishable in the ribbons, which were spun using higher wheel velocity. In order to find differences in orientation of grains, which were formed from both sides, the pole figures were measured from the contact as well as free side. Figure 5 presents comparison of two pole figures {110} and {100} measured from both side of the Cu-Al-Ni-Ti ribbon spun at 26 m/s. The crosses marked in the pole figures represent the poles of {111}<112> sheet texture component. The grains at the contact side showed very weak texture. Maximum of the pole density did not exceed 2 levels. Two sheet textural components {112}<111> and {111}<112> were identified. However, almost 94% grains were randomly oriented. Similar amounts were obtained in the ribbons spun using 12 and 19 m/s. In contrast to that, total volume of preferentially oriented columnar grains crystallized at zone, close to the free side, was 52%. Two sheet components {112}<111> and {110}<110> disappeared. Mainly, grains were oriented along the <111> fibre (43% of total volume) and the {111}<112> sheet textural components (9% of total volume). It can be concluded that the most representative texture characteristic reveals the columnar grains extended from the middle of the cross-section up to the free side of the ribbon. Considering that fact, influence of the wheel velocity on grains orientation is

discussed only for measurement done for the free side of all ribbons. Figure 6 presents differences in texture, which was formed dependently on the wheel velocity. For convenience, only a set of the 110 pole figures measured for the Cu-Al-Ni-Mn ribbons is shown in Figure 6a whereas Figure 6b represents a set of the {100} registered for the Cu-Al-Ni-Ti ribbons. Table 2 contains the volume fraction calculated from the ODF. In general, the ribbons of both alloys reveal similar grains orientation to that reported for the Cu-A-l-Ni alloy by Morawiec et al. [11] and the Cu-Al-Ni-Ti alloy by Goryczka [10]. Mainly, one fibre <100> and two sheet textural components {100}<001> or/and {100}<011> were identified. However, the increase of the wheel velocity caused tilting of the columnar grain axis. The arrows marked in Figure 6a for the Cu-Al-Ni-Mn ribbons spun using 12 m/s or 19 m/s, show 15 degrees tilt of the {100}<011> component in RD direction. The <100> and {100}<001> components did not changed their positions. However, they were scattered around their positions about 8 degrees in TD direction. It can be caused by turbulences of melt flow on the wheel surface. Consequently, the columnar grains formed shape of ”palm tree”, which were observed in both alloys (Figure 4b). In a case of the ribbon spun using 26 m/s the {100}<001> sheet textural component completely disappeared and both textural components: <100> and {100}<011>, were tilted of 24 degrees. Increase of the wheel velocity for manufacturing the ribbons caused higher scattering of the poles than it was observed for the Cu-Al-Ni-Ti ribbons. For applied wheel speeds of 12 m/s and 19 m/s, significant spread around the poles of the sheet components was noticed. This scattering of the poles is marked with the arcs showing direction of their tilting from the original position. In the Cu-Al-Ni-Ti ribbon spun with 26 m/s tilting was such strong that 42,3% of the grain were preferentially oriented along the <111> fibre texture and 8,9% along the {111}<112> sheet texture component. The {100}<001> and {100}<011> components vanished completely.

a) b)

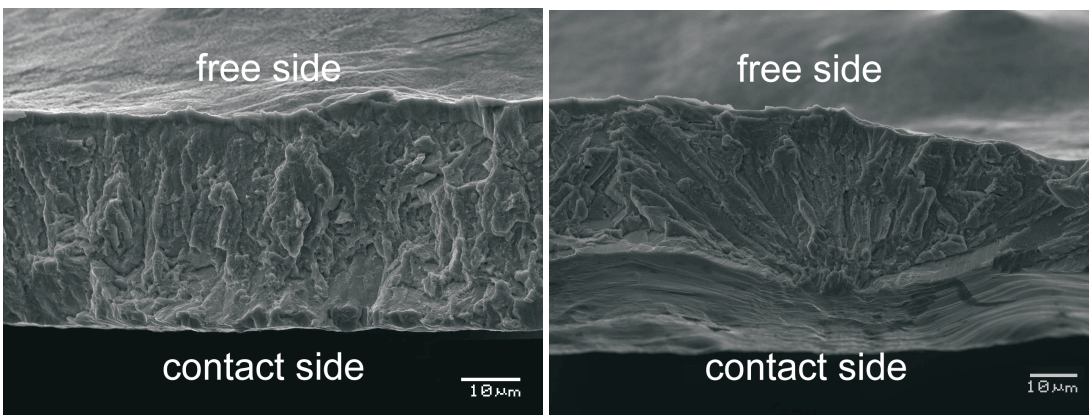

Fig. 4. SEM images of fracture perpendicular on the cross-section of the Cu-Al-Ni-Ti ribbons spun using wheel velocity of 12 m/s (a) and 26 (b)

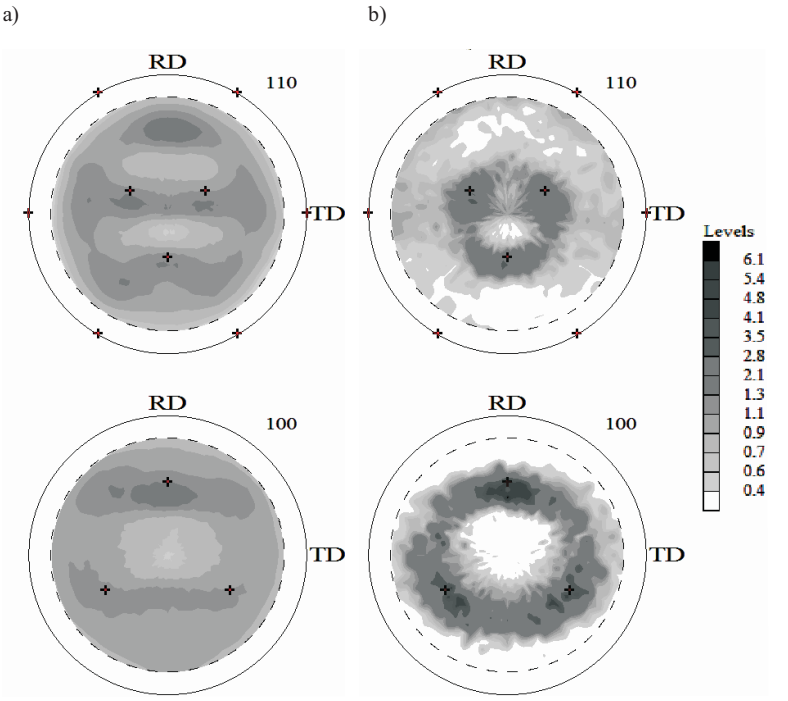

Fig. 5. The {110} and {100} pole figures registered from: (a) contact side and (b) free side for the Cu-Al-Ni-Ti ribbon spun with speed of 26m/s

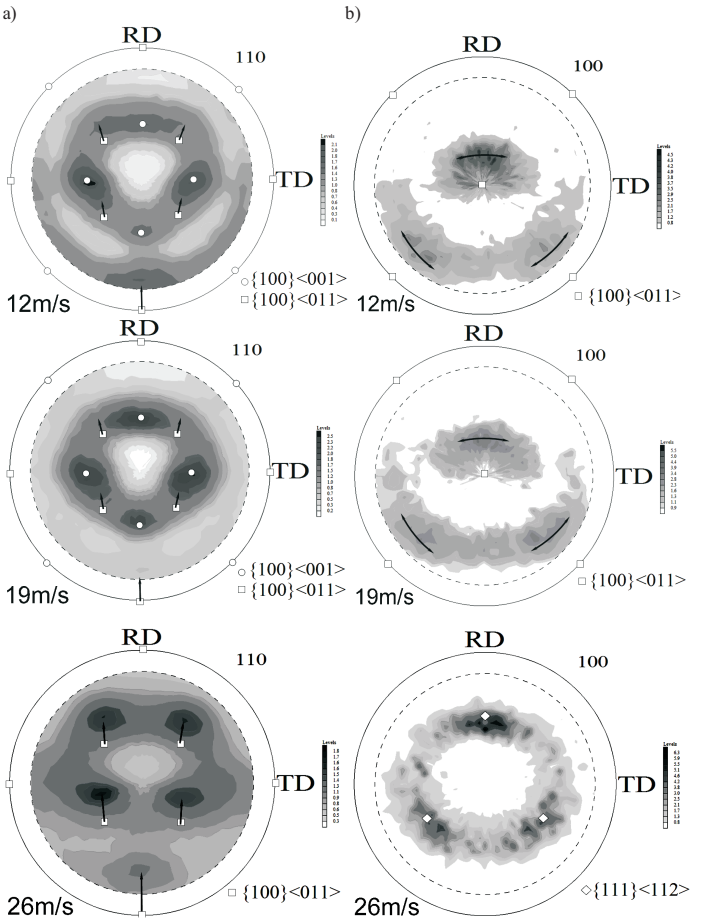

Fig. 6. Set of the {110} pole figures measured for the Cu-Al-Ni-Mn (a) and the {100} for Cu-Al-Ni-Ti ribbons (b) produced with various wheel velocity

TABLE 2

Volume fractions of the grains oriented along identified texture components

Alloy	Wheel velocity [m/s]	Volume fraction [%]				
		<100>	<111>	{100}<001>	{100}<011>	{111}<112>
Cu-Al-Ni-Mn	12	22,5	–	14,0	10,2	–
	19	21,3	–	13,3	9,5	–
	26	10,8	–		–6,9	–
Cu-Al-Ni-Ti	12	24,6	–	13,5	–	–
	19	19,0	–	–	10,6	–
	26	–	42,3	–	–	8,9

3.3. Shape memory effect

The main condition for shape memory effect appearance is the reversible martensitic transformation. All ribbons revealed that they can transform from the parent phase to the martensite during cooling and from the martensite to the parent phase, when they were heated. Applying additional constant stress during thermal cycling induces two way shape memory effect.

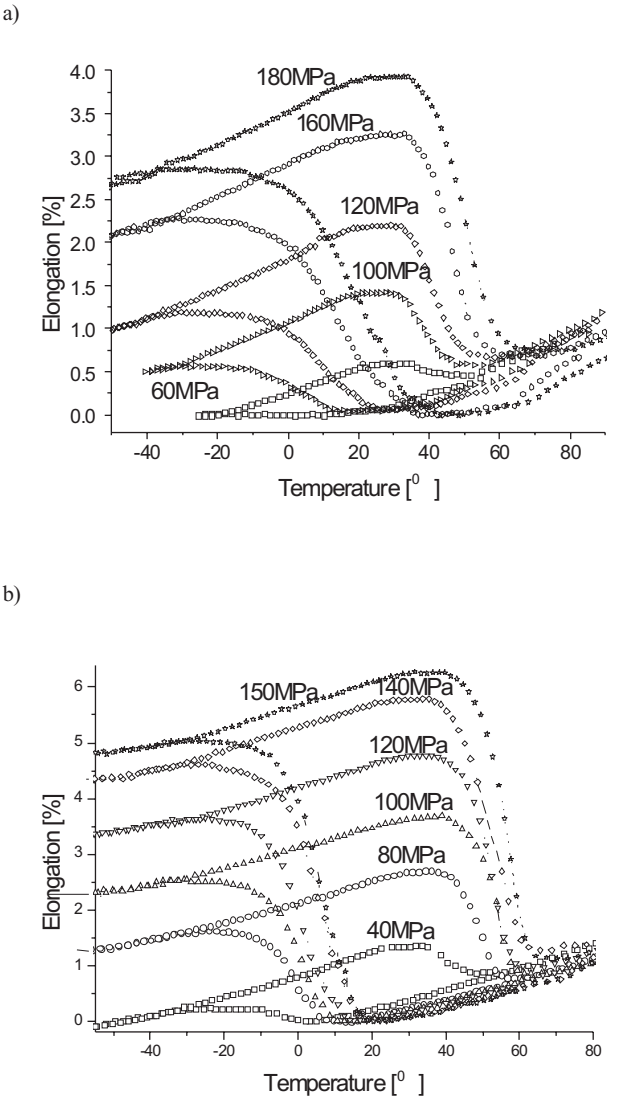

Fig. 7. The shape recovery versus increase of stress for the Cu-Al-Ni-Mn (a) and the Cu-Al-Ni-Ti (b) ribbons spun applying wheel velocity of 19 m/s

Figure 7 shows first cycles obtained for the ribbons spun applying the wheel velocity of 19m/s. The maximum stress, which can be reached avoiding plastic deformation, is 180MPa and 150Pa for the Cu-Al-Ni-Mn and ribbons, respectively. However, the thermal loops remain open beginning from 120 MPa for Cu-Al-Ni-Mn and 100 MPa for Cu Al-Ni-Ti, consequently, permanent elongation appeared. It means that the shape of the ribbons was not completely recovered and some percentage of the elongation remained. In order to close the thermal loops and achieve full recovery of the shape, additional cycles were repeated keeping the same value of stress. During such cycling thermo-elastic martensite is formed and its heating above A_f temperature results in the reverse martensitic transformation occurrence. In consequence, parent phase can be again transformed to the martensite in next thermal cycle. An example of the shape recovering for the Cu-Al-Ni-Ti ribbon spun with 26 m/s is shown in Figure 8. After two cycles under 40 MPa permanent elongation equals zero and shape of the ribbon is fully recovered. However, after exceeding of the yield stress the martensite is plastically deformed and further repetition of cycles for receiving of the original shape is useless. Each next cycle, done applying 60 MPa, increased plastic deformation.

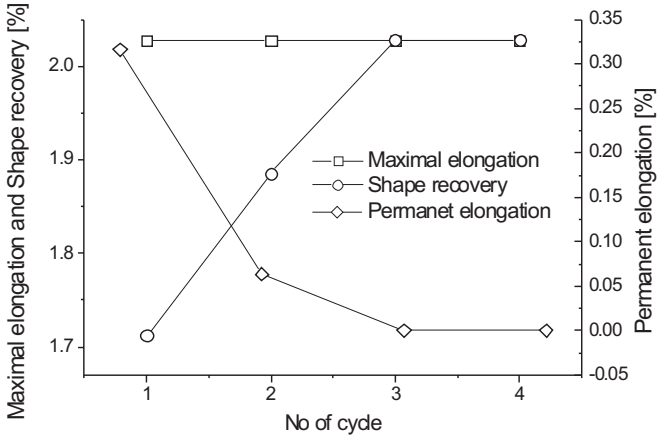

Fig. 8. The shape recovery for the Cu-Al-Ni-Ti ribbon spun with 26 m/s after cycling under constant tensile stress of 40 MPa

For the convenience, maximal recovered elongation was calculated for closed thermal loops and shown versus change of the tensile stress in Figure 9. The ribbons of Cu-Al-Ni-Mn alloys, spun with wheel velocity of 12 m/s or 19 m/s, revealed comparable shape recovery (Figure 9a). However, starting from 120 MPa the curves slightly differ. Maximal elongation, which can be achieved from the ribbon spun with 12 m/s was 5.8% at tensile stress of 200 MPa. This value lowered down to 4,9% for the ribbon spun using 19 m/s. It can be due to the fact that the volume fraction of grains oriented along <100> as well as {100}<001> components decreased. Both textural components are highly favorable for the martensitic plate formation. Increase the wheel velocity up to 26 m/s lowers the tensile stress down to 80MPa simultaneously receiving 3,6% recoverable elongation. It can be caused due to significant decrease of volume fraction of grains oriented along <100> textural component.

a)

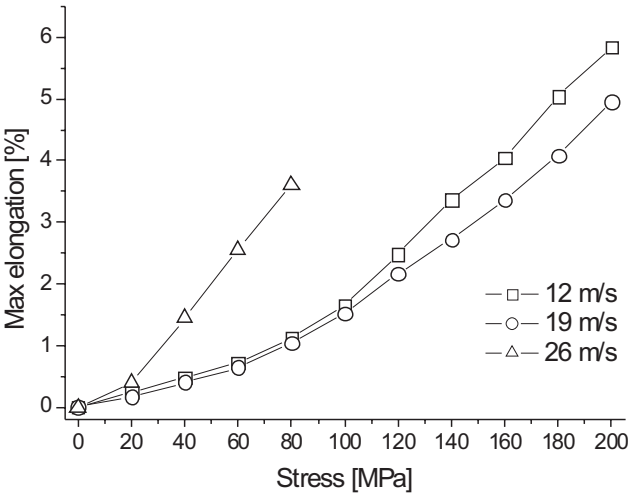

b)

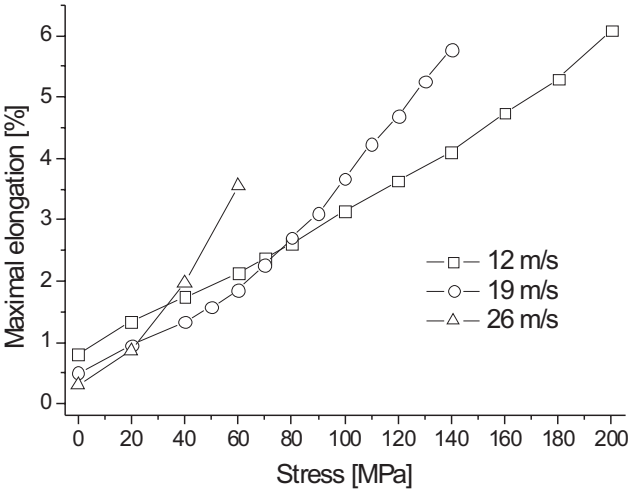

Fig. 9. The shape recovery versus increase of tensile stress for (a) Cu-Al-Ni-Mn and (b) Cu-Al-Ni-Ti ribbons

Two way shape memory effect, with the recovery up to 0.9%, was observed in Cu-Al-Ni-Ti ribbons without applying any stress (Figure 9b). It can be a result of relatively high amount of the grains orientated along {100} plane. Maximum of elongation, which can be received from the Cu-Al-Ni-Ti ribbons was around 6,2%. Application of higher wheel speed (19m/s) caused decrease

of the volume fraction of the grains oriented along the fibre texture. In consequence, the maximum recoverable elongation decreased down to 5,8%. However, decrease of the wheel velocity allowed to lower the tensile stress from 200 MPa down to 140 MPa for the ribbons spun with 19 m/s. In case of the ribbon spun applying 26m/s dominant texture component was the fibre <111>. Due to the plastic deformation, which appeared at 60MPa the total elongation increased over 3,5%. However, less than 2,0% of elongation could be recovered as a result of the shape memory effect. It is worthy to notice that the {111}<112> texture reveals a direction slightly rotated at the {111} plane from the {111}<110> slip system, which is characteristic for face centered cubic structure of parent phase. Presence of the <111>{112} and <111> textures cause plastic deformation at relatively low tensile stress. The results are in a good agreement with that obtained for polycrystalline Cu-Al-Ni melt spun ribbons and presented by Euken et al [5]. The most favorable direction for achieving the maximal shape recovery, in creation of the 18R martensite, is <100> direction. In a case of the 2H martensite [110] direction was found to be promoted for shape recovery [16]. However, the 2H martensite was locally identified in both alloys and its amount did not exceed of a few percent [12]. Thus the main responsibility for the shape recovery is in a charge of the formation of the 18R. Considering the shape recovery one has to remember that the identified textural components were perpendicular to the surface of the ribbons. However, the texture components <100> and {100}<001> guarantee that one of the equivalent [100] direction can be parallel to the external tensile stress. Also the [110] direction is supportive for the 18R and this direction can be find from the {100}<011> texture as parallel to direction of applied stress. Owing to comparable high total amount of the grains oriented in mentioned textural components, existing in the ribbons spun with 12 m/s or 19 m/s, relatively high degree of the shape recovery was achieved.

4. Conclusions

- Applying the wheel velocity from 12 up to 26 m/s allows obtaining melt-spun ribbons of Cu-Al-Ni-Ti and Cu-Al-Ni-Mn alloys with the martensitic transformation occurring in the thermal range between -50°C and +55°C.
- Increase of the wheel velocity causes tilting of the columnar grains as well as decreasing of the amount of preferentially oriented grains.
- The ribbons produced using wheel speed of 12 m/s or 19 m/s reveal similar transformation behavior and comparable shape recovery.
- Maximal elongation which can be recovered under constant tensile stress, applied along the ribbon, is 5,8% and 6,2% for the Cu-Al-Ni-Mn and Cu-Al-Ni-Ti alloys, respectively.
- Presence of the favorable textural components significantly decreases the tensile stress (100MPa), which is needed to induce two way shape memory effect.

REFERENCES

[1] K. Otsuka, T. Nakamura, K. Shimizu, Trans Jap Inst Met. **15**, 200-210 (1974).

[2] G. J. Hall, S. Govindjee, P. Sittner, V. Novak, Int J. Plast. **23**, 161-182; (2007).

[3] M. Tokonami, K. Otsuka, K. Shimizu, Y. Iwata, I. Shibuya, Proc. of International Conference of Martensitic Transformation ICOMAT 638-644 (1979).

[4] K. Bhattacharya, R. V. Kohn, Acta Mater. **44**, 529-542 (1996).

[5] S. Euken, J. Hirsch, Mat. Sci. Forum **56-58**, 487-492 (1990).

[6] K. Otsuka, C. M. Wayman, Shape Memory Materials, Cambridge University Press, 1998.

[7] J. Pons, L. Jordan, J. P. Morniroli, R. Portier, J. Phys. IV, C3-C293 (1995).

[8] J. Dutkiewicz, T. Czeppe, J. Morgiel, Mater. Sci. Eng. **A 273-275**, 703-707 (1999).

[9] H. Morawiec, J. Lelątko, D. Stróż, M. Gigla, Mater. Sci. Eng. **A 273-275**, 708-712 (1999).

[10] T. Goryczka, H. Morawiec, Mat. Sci. Engin. **A 378**, 248-252 (2004).

[11] H. Morawiec, T. Goryczka, J. Lelątko, D. Stróż, M. Gigla, P. Tkacz, Arch. Mater. Sci. **24**, 5 (2003).

[12] C. Segui, T. Goryczka, J. Pons, E. Cesari, H. Morawiec, Proc. of the International Conference on Solid-Solid Phase Transformation (JIMIC-3), 1072-1075 (1999).

[13] J. Malarrïa, C. Elgoyhen, Ph. Vermaut, P. Ochin, R. Portier, Mat. Sci. Eng. **A 438-440**, 763-767 (2006).

[14] K. Pawlik, P. Ozga, LaboTex: The Texture Analysis Software, Göttinger Arbeiten zur Geologie und Paläontologie, SB4, (1999).

[15] H. Morawiec, D. Stróż, T. Goryczka, D. Chrobak, Scripta Mater. **35**, 485-490 (1996).

[16] H. Funakubo, Shape memory alloys; Gordon and Breach Science Publishers 38, (1987).

Received: 10 January 2009.